Monte Carlo Modeling and Analysis of Drell – Yan Events at LHC Energies Using MadGraph

By:
Antonia Atanasova Kushleva
Faculty number: 8PH0760001
Sofia, September 2025

Contents:

- Overview of Standard Model Particles
- High Energy Physics Experiments - LHC
- Drell – Yan Processes
- Monte Carlo Setup
- Experimental Work
- Conclusion

Overview of Standard Model Particles

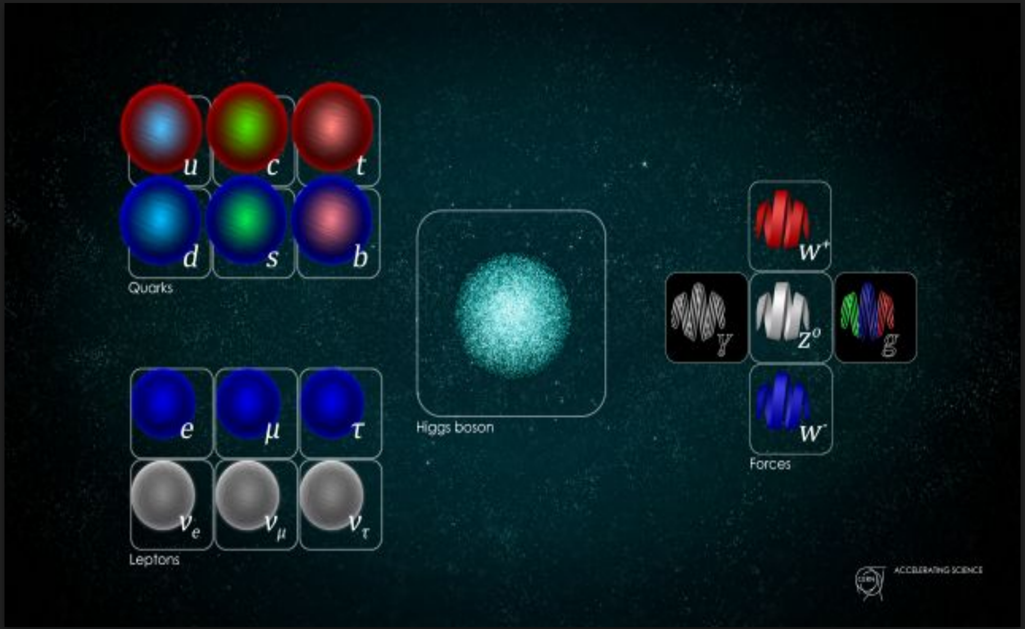

The particles of the Standard Model organized by type and interaction.

High Energy Physics - LHC

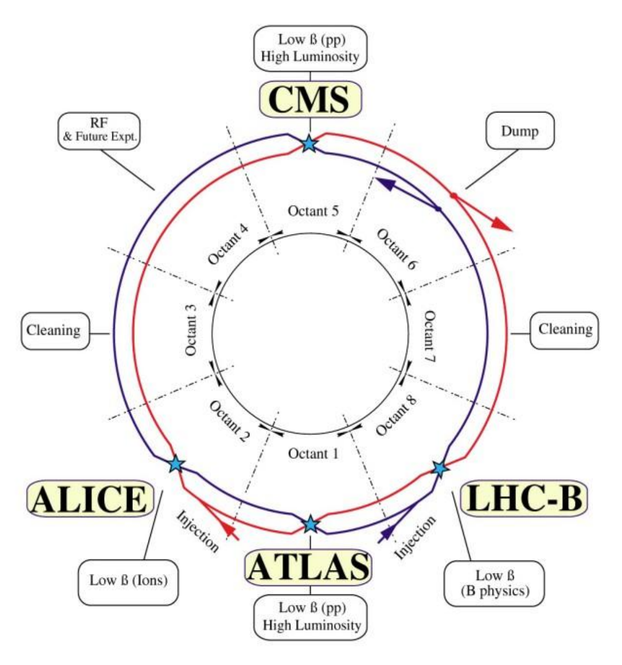

Schematic layout of the Large Hadron Collider (LHC) at CERN, showing its 27 – kilometer ring and the main experimental sites

HEP Experiments at LHC:

- ATLAS and CMS: Investigate the Standard Model (SM) physics, Higgs boson production and properties, and eventual new physics beyond the SM, in particular Supersymmetry, CP violations and more.
- LHCb: Specializes in studying heavy flavor physics and CP violation.
- ALICE: Focuses on heavy-ion collisions and the properties of quark-gluon plasma.

Drell – Yan Processes

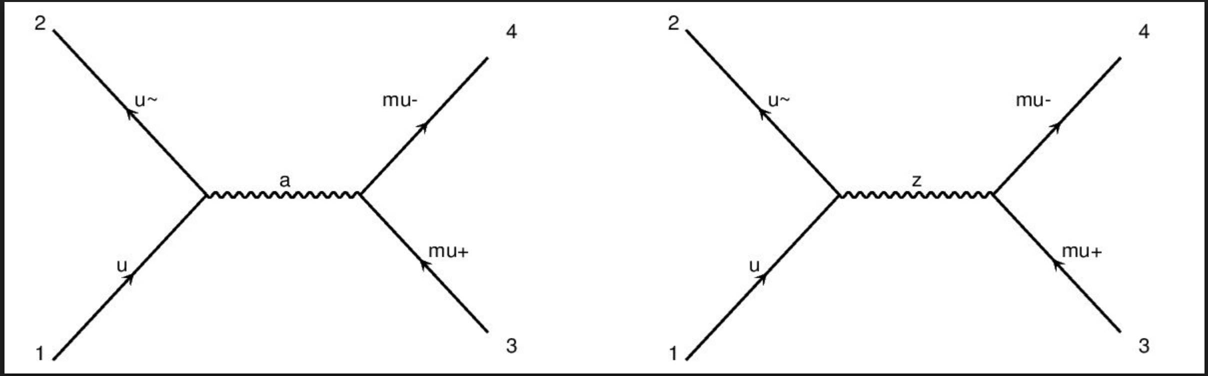

The Drell – Yan Process.
On left the process is mediated by a photon, on right through Z-boson.

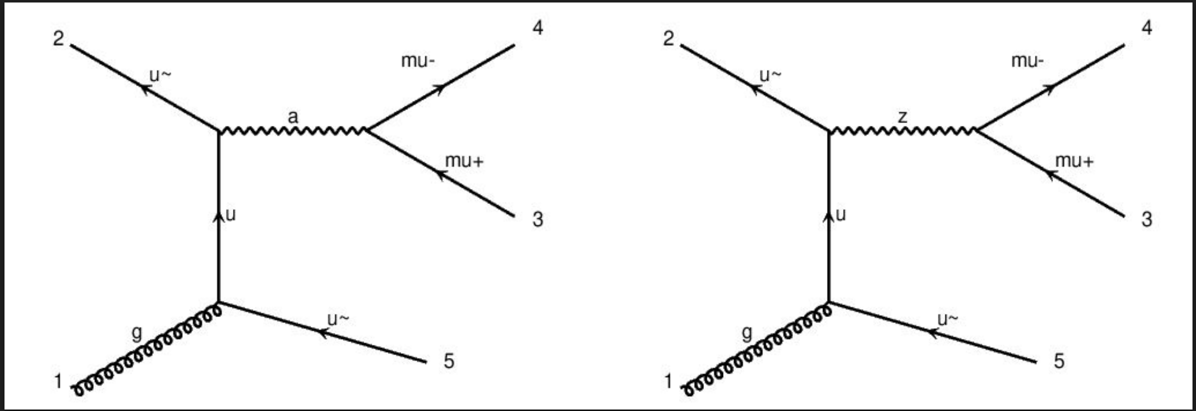

The Drell – Yan Process with one additional jet.

Monte Carlo Simulations Of The Drell – Yan Process Using Generators MadGraph5 and PYTHIA8

Monte Carlo generators:

- MadGraph5_aMC@NLO, version 2.9.21 (parton level generation)
- PYTHIA8 (parton showers, hadronization, and decays)

Generated processes:

- $p\ p \rightarrow \mu^+\ \mu^-$
- $p\ p \rightarrow \mu^+\ \mu^-$ + jets
- $p\ \bar{p} \rightarrow \mu^+\ \mu^-$
- $p\ \bar{p} \rightarrow \mu^+\ \mu^-$ + jets
- $p\ p \rightarrow \mu^+\ \mu^- / Z$
- $p\ p \rightarrow \mu^+\ \mu^- / Z$ + jets

- Generation with MadGraph and Pythia->LHE file->The software frame CMSSW->ROOT format->TLorentzVector

Invariant Mass Distributions in Drell–Yan

The Drell – Yan process occurs via the s-channel and is characterized by the Mandelstam variable, s as follows:

$$s = (p_3 + p_4)^2 = m_3^2 + m_4^2 + 2E_3E_4 - 2\vec{p}_3 \cdot \vec{p}_4$$

Where:

- p3 and p4 are the four-momenta of the outgoing particles,
- m3 and m4 are their rest masses
- E3 and E4 are their corresponding energies,
- $\vec{p}_3$ $\vec{p}_4$ are their three-momenta (spatial parts of the four-momenta).

In Drell – Yan, when a Z boson is produced and decays into two muons, it shows up as a peak in the di-muon invariant mass. To describe this peak, we use the Breit – Wigner function, which is widely used in high energy physics to model the resonances.

The formula that we use is:

$$f(m) = \frac{1}{2\pi} \cdot \frac{\Gamma}{(m - m_0)^2 + \Gamma^2/4}$$

Here:

- m is the measured mass,
- m0 is the expected mass (the mass of the Z boson),
- Γ (Gamma) is the expected width of the mass peak. The width of the peak is reciprocal to the time of life of the particle. As narrow is the peak, as longer lives the particle and vice versa.

Invariant Mass Distributions in Drell–Yan

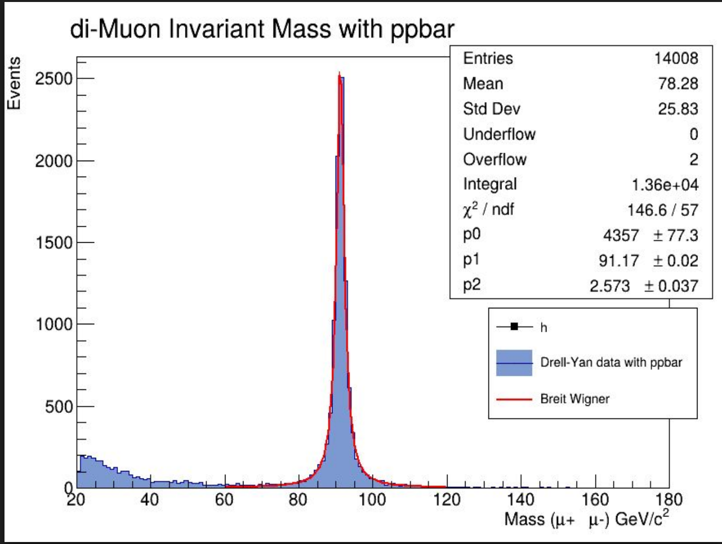

Di-muon mass spectrum from $\bar{p}p$ collisions. The clear peak at 91.17 GeV shows Z boson production. The red curve is the Breit – Wigner fit. The width of the peak (2.57 GeV) shows how long the Z boson lives.

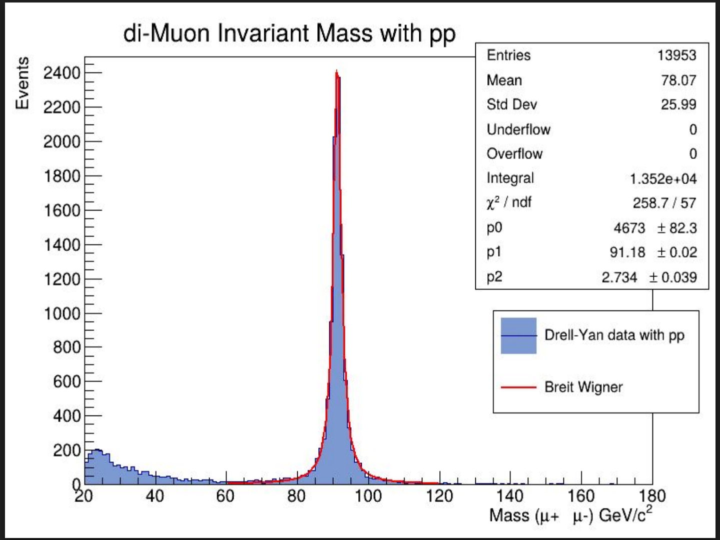

Mass distribution of muon pairs from pp collisions. There is a broad bump around 20 GeV from general Drell – Yan events and a clear peak at 91.18 GeV from Z bosons. The Z peak is slightly wider here (2.73 GeV) than in $\bar{p}p$ collisions.

Parameter	$\bar{p}p$ collisions	pp collisions	PDG (2025)
Mass (GeV)	91.17 ± 0.02	91.18 ± 0.02	91.1880 ± 0.0020
Width (GeV)	2.573 ± 0.037	2.734 ± 0.039	2.4955 ± 0.0023

Comparison of measured Z boson mass and width from $\bar{p}p$ and pp collisions with PDG values.

Polar angle θ = angle (Z, Y)

η-Pseudorapidity

$$\eta = -\ln\left(\tan\frac{\theta}{2}\right)$$

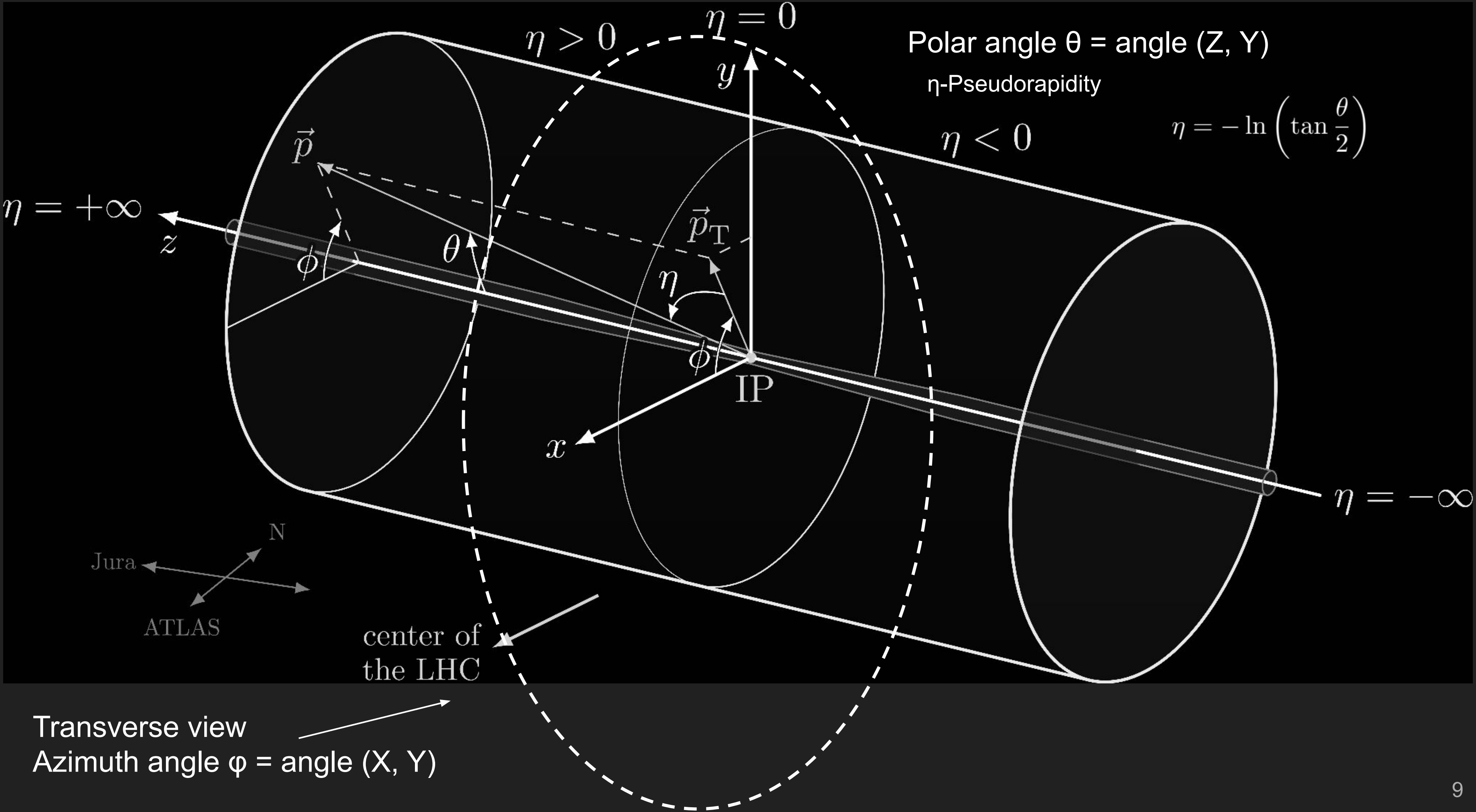

Transverse view

Azimuth angle φ = angle (X, Y)

Azimuthal Angle Distribution

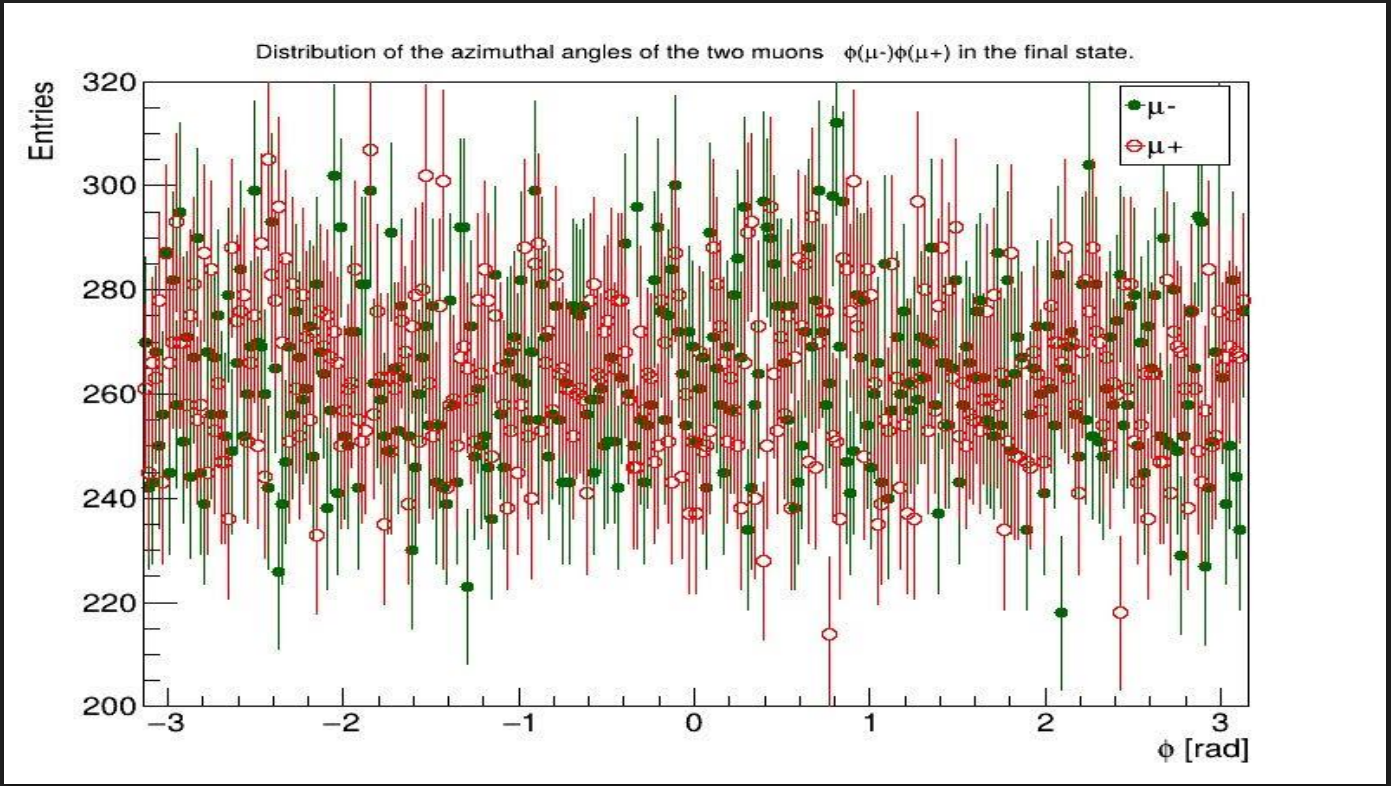

Distribution of the azimuthal angles of the two muons in the final state.
The green full circles depict for negatively charged muon, and the red empty once - for the positively charged one.

Dimuon pT vs. pz

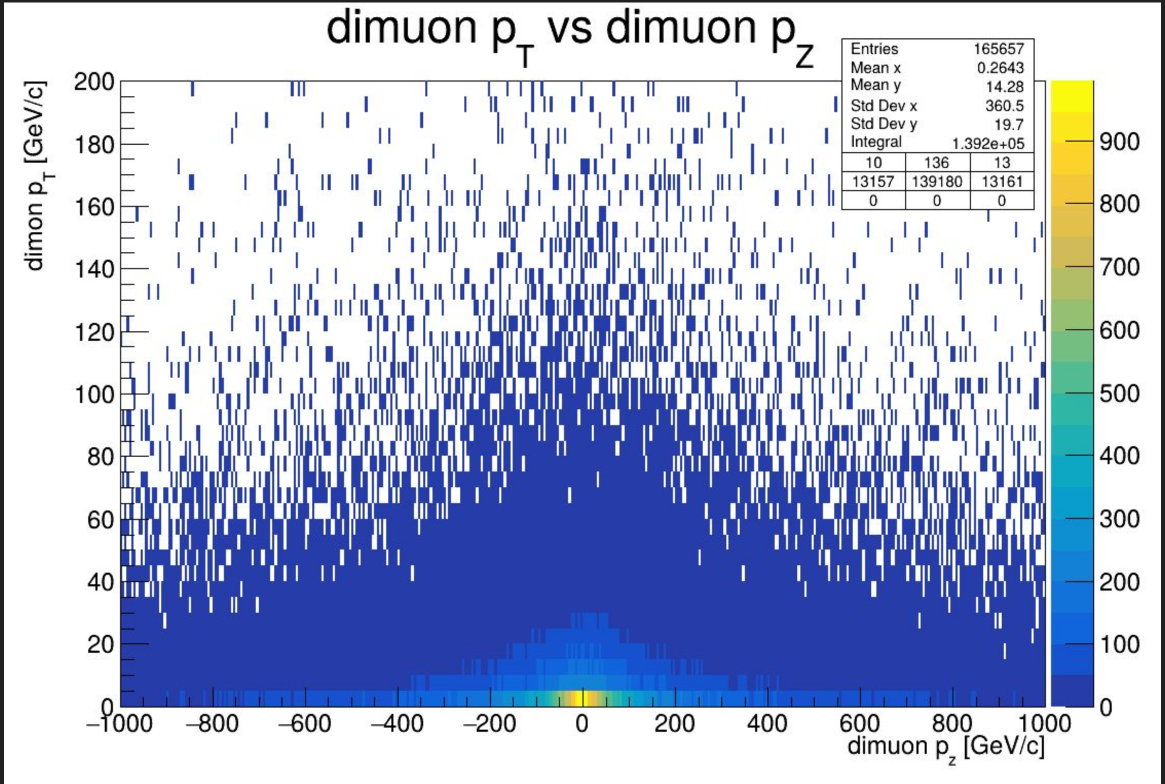

2D histogram of dimuon transverse momentum pT versus longitudinal momentum pz .

Dimuon pT vs. Azimuthal Angle Difference Δϕ

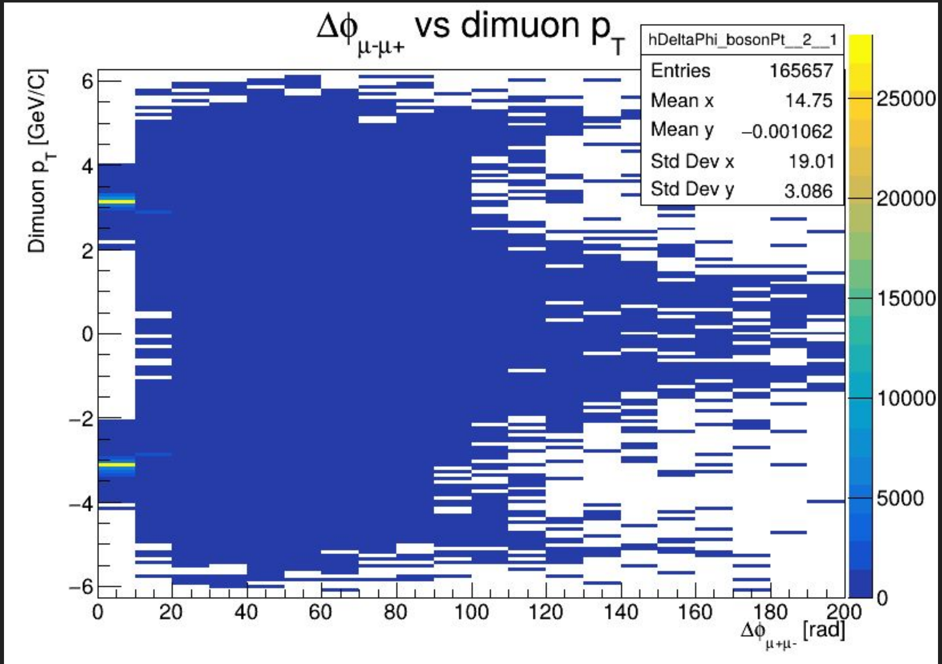

Rebinned 2D histogram of Δϕμ+μ− and Dimuon pT.
The central peak represents about 25% of the events.

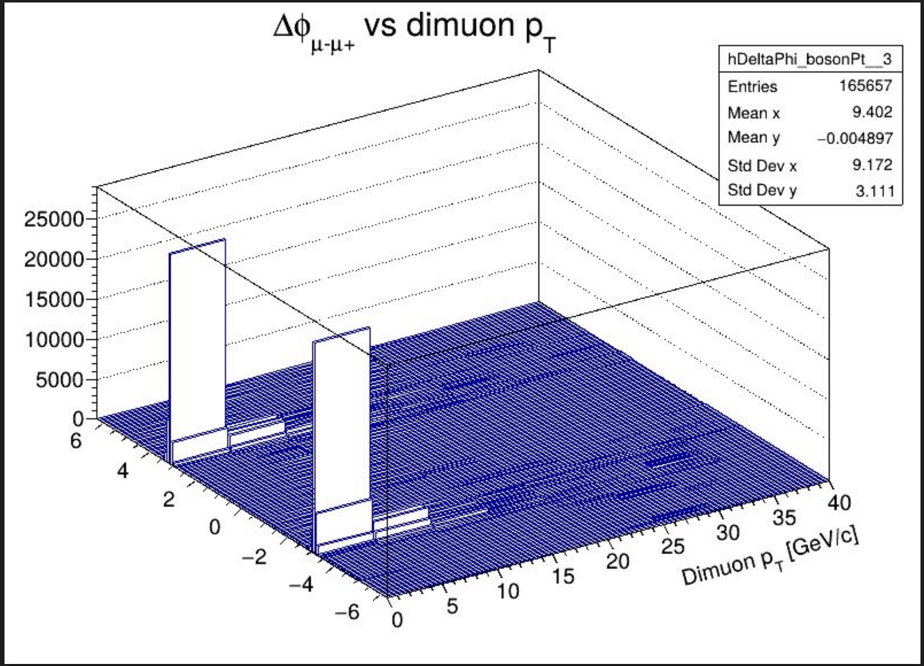

3D surface plot that shows the difference in the azimuthal angles Δϕμ+μ− vs the transverse momentum pT of the dimuon system.

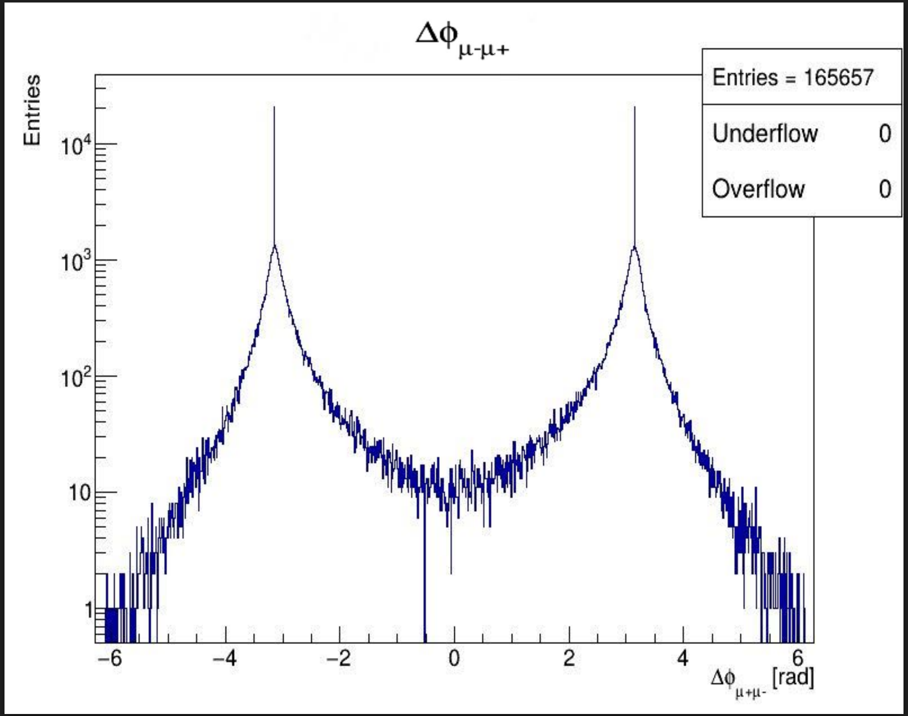

Distribution of the azimuthal angle difference Δϕμ+μ− . The sharp peaks near ±π show that muons are usually emitted in opposite directions.

We want to investigate what portion of the muon pairs are born centrally and what portion of them are born with some boost and therefore the two muons do not scatter back to back.

Left peak: 20 855 events

Right peak: 20 734 events

$$\frac{41589}{165657} \approx 0.251 \Rightarrow 25.1\%$$

25% of the collisions are central, where the muons come out in opposite directions. The other 75% of the events are more spread out, meaning the muons are not exactly back-to-back and there is some boost.

Distribution of cos θ∗ in the Collins – Soper frame for Drell – Yan events

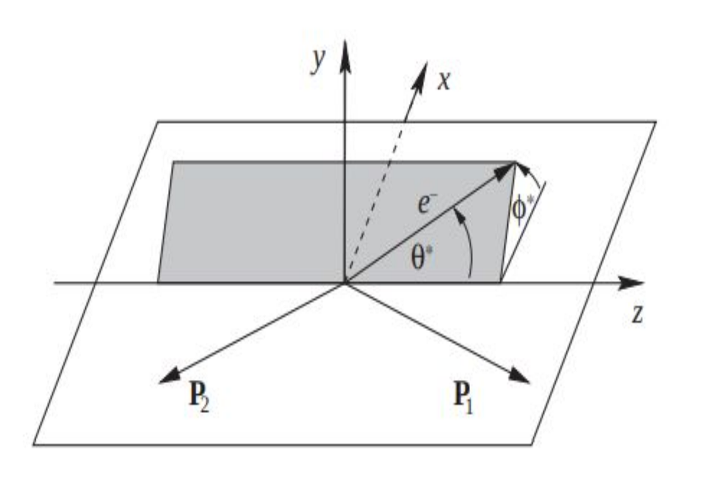

The Collins–Soper reference frame. The angle θ∗, describes the orientation of the negatively charged lepton relative to the incoming quark direction.

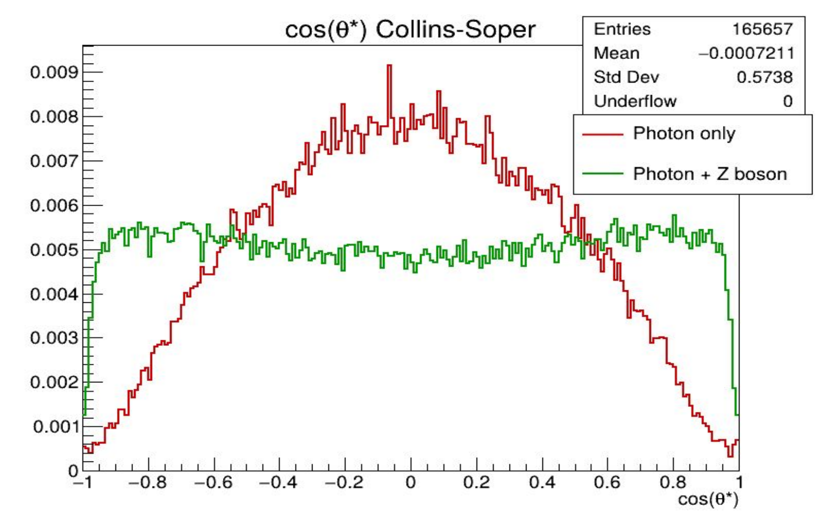

When the process is only through the photon (shown in red), we observe a symmetric distribution with more events around cos(θ∗) = 0, i.e., θ∗ = 90◦, and far fewer events as cos(θ∗) approaches 1. However, when the process is mediated by both the Z boson and the photon, we see a completely different behavior, the distribution is nearly uniform with a slight dip in the middle. This is why we study the dependence of cos(θ∗) as a function of the invariant mass.

Cos(θ∗) vs. Dimuon Invariant Mass

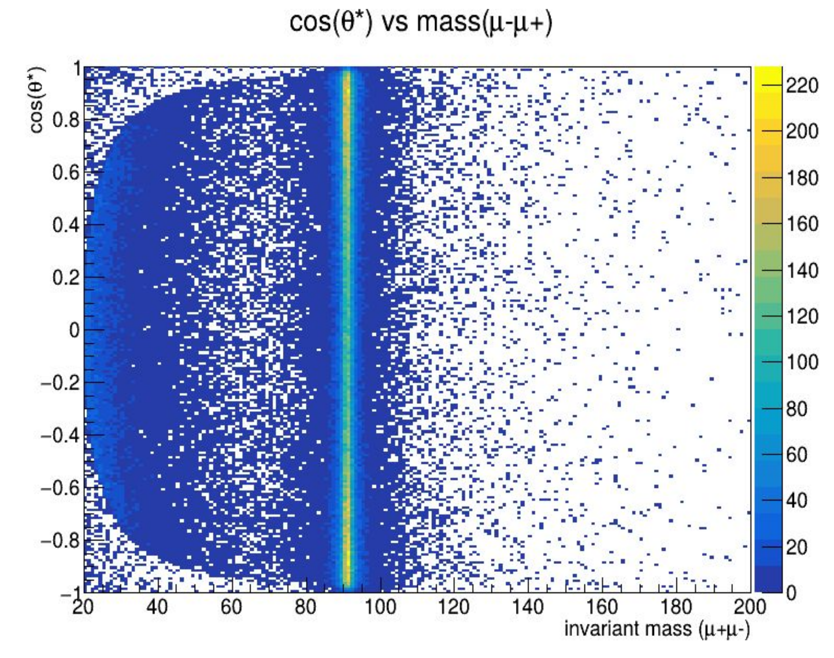

2D histogram of cos(θ∗) versus dimuon invariant mass mμ+μ−.

3D view of cos(θ∗) versus mμ+μ− , showing the density of events across different angular and mass values.

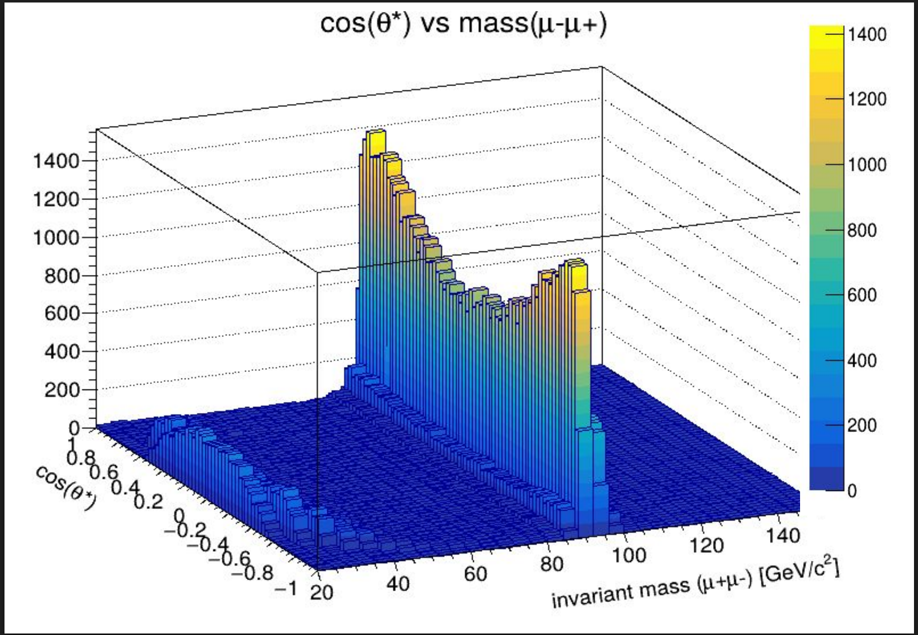

Conclusion:

In this thesis, the Drell – Yan process is simulated using Monte Carlo generators MadGraph5 and Pythia8. The kinematic properties of the final states consisting of two muons are studied. Further studies using the Collins – Soper frame reveal characteristic structures depending on whether the interaction is mediated by a real massive particle or a virtual photon. This difference can be used in future analyses as an additional criteria for event selection.

References:

[1] S. Drell and T.-M. Yan. "Massive Lepton-Pair Production in Hadron-Hadron Collisions at High Energies". In: Physical Review Letters 25 (1970), pp. 316–320. doi:10.1103/PhysRevLett.25.316.

[2] Johan Alwall et al. "MadGraph 5: Going Beyond". In: Journal of High Energy Physics 2011.6 (2011), p. 128. doi: 10 . 1007 / JHEP06(2011) 128. url: https ://doi.org/10.1007/JHEP06(2011)128.

[3] J. Alwall et al. "The automated computation of tree-level and next-to-leading order differential cross sections, and their matching to parton shower simulations". In: Journal of High Energy Physics 2014.7 (2014), p. 79. doi://10.1007/JHEP07(2014)079.

[4] T. Sjöstrand et al. "An introduction to PYTHIA 8.2". In: Computer Physics Communications 191 (2015), pp. 159–177. doi: 10.1016/j.cpc.2015.01.024.

[5] Johan Alwall et al. "Comparative study of various algorithms for the merging of parton showers and matrix elements in hadronic collisions". In: Eur. Phys. J. C 53 (2008), pp. 473–500. doi: 10.1140/epjc/s10052-007-0490-5. arXiv: 0706.2569 [hep-ph].

[6] Daniel Dominguez. Particles of the Standard Model of Particle Physics. Image courtesy of CERN. 2015. url: https : / / home . cern / resources / image / physics / infographics-gallery.

[7] CERN. LHC layout. https://cds.cern.ch/record/841573. Accessed: 2025-05-25. 1997.

References:

[8] Markus Lichtnecker. “Determination of s via the Differential 2-Jet-Rate with ATLAS at LHC”. Accessed: 2025-05-22. PhD thesis. Ludwig-Maximilians-Universität München, 2011. url: https : / / repository . cern / records / b469v - ey032 /preview/Lichtnecker_Markus.pdf.

[9] Ryan Atkin. “Review of jet reconstruction algorithms”. In: Journal of Physics: Conference Series 645.1 (2015), p. 012008. doi: 10.1088/1742-6596/645/1/012008.

[10] Torbjörn Sjöstrand, Stephen Mrenna, and Peter Skands. “PYTHIA 6.4 Physics and Manual”. In: Journal of High Energy Physics 2006.05 (2006), p. 026. doi:10.1088/1126-6708/2006/05/026.

[11] René Brun and Fons Rademakers. “ROOT – An Object Oriented Data Analysis Framework”. In: Proceedings of the AIHENP’96 Workshop, Lausanne. Vol. 389.1996, pp. 81–86.

[12] Particle Data Group, S. Navas, et al. “Review of Particle Physics”. In: Phys. Rev.D 110 (1 July 2024). and 2025 update, p. 030001. doi: 10.1103/PhysRevD.110.030001. url: https://pdg.lbl.gov/

[13] J. C. Collins and D. E. Soper. “Angular Distribution of Dileptons in High-Energy Hadron Collisions”. In: Physical Review D 16 (1977), p. 2219. doi: 10 . 1103 /PhysRevD.16.2219.

[14] et al. D0 Collaboration V. Abazov. “Measurement of sin2 θlept eff and Z-light quark couplings using the forward-backward charge asymmetry in p ̄p → Z/γ∗ → e+ events with L = 5.0 fb−1 at √s = 1.96 TeV”. In: Phys. Rev. D 84 (2011), p. 012007. doi: 10.1103/PhysRevD.84.012007. arXiv: 1104.4590 [hep-ex]. url: https://doi.org/10.1103/PhysRevD.84.012007.

Thank you for the attention!

Antonia Atanasova Kushleva
Faculty number: 8PH0760001
Sofia, September 2025

Questions From the Reviewer and Answers.

1. How did you choose the bin width of the histograms and the Y-axis range of the plot in Figure 7.2?

First, I chose the bin width to be 1 GeV without confirming with calculations. I chose it, based on my supervisor's evaluation, since she knows from previous experience that the best width is 0,6 x expected width (2,1) ≈ 1,2600 which we round to 1.

Further we confirm this using two formulas:

$$w_{bin} = \frac{3.49\,\sigma}{N^{\frac{1}{3}}}$$ where σ is the standard deviation, N the sample size

(Scott, D. 1979. *On optimal and data-based histograms.* Biometrika, 66:605-610.)

$$w_{bin} = \frac{2\,IQR}{N^{\frac{1}{3}}}$$ where IQR (interquartile range) is the distance between the 25th and 75th percentiles (= the middle range containing half of the sample)

(Izenman, A. J. 1991. *Recent developments in nonparametric density estimation.* Journal of the American Statistical Association, 86(413):205-224.)

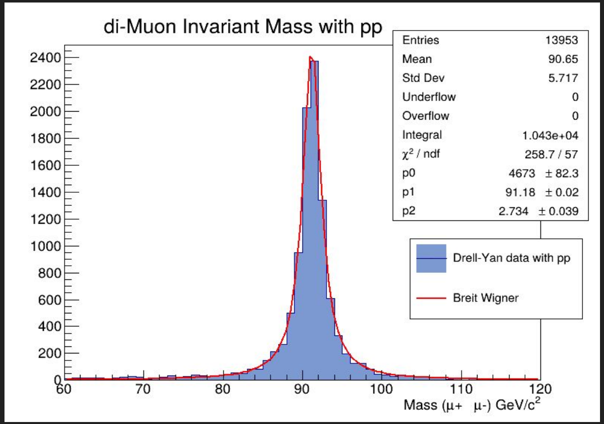

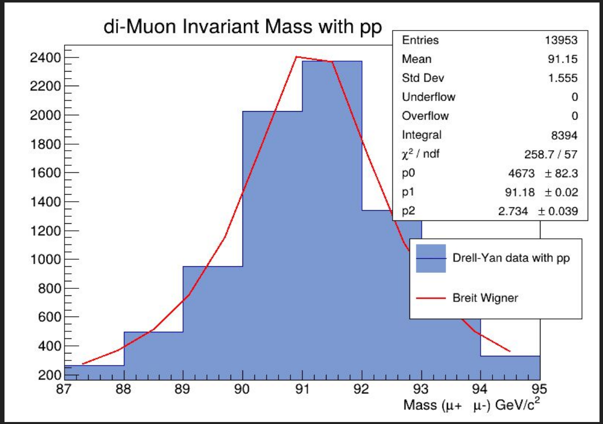

Formula 1:

$$w_{bin} = \frac{3.49\,\sigma}{N^{\frac{1}{3}}}$$

where σ is the standard deviation, N the sample size

(Scott, D. 1979. *On optimal and data-based histograms*. Biometrika, 66:605-610.)

We calculate the bin width:

$$W_{bin} = \frac{3.49\,\sigma}{N^{1/3}}$$

Substituting the values:

$$W_{bin} = \frac{3.49 \times 5.717}{\sqrt[3]{13953}}$$

$$W_{bin} = \frac{19.952}{24} \approx 0.83 \approx 1$$

Formula 2:

$$w_{bin} = \frac{2\,IQR}{N^{\frac{1}{3}}}$$

where IQR (interquartile range) is the distance between the 25th and 75th percentiles (= the middle range containing half of the sample)

(Izenman, A. J. 1991. *Recent developments in nonparametric density estimation*. Journal of the American Statistical Association, 86(413):205-224.)

We calculate the bin width using the IQR method:

$$W_{bin} = \frac{2\,IQR}{N^{1/3}}$$

Substituting the values:

$$W_{bin} = \frac{2 \times (95 - 87)}{\sqrt[3]{8394}}$$

$$W_{bin} = \frac{16}{20.41} \approx 0.78 \approx 1$$

2. What is the meaning of the sign of the Azimuthal Angle Difference defined in Chapter 7? Did you order the muons in the muon pairs in a specific manner, before subtracting their azimuthal angles?

When we ordered the muons in the muon pairs, we chose the negatively charged muon as the first one.